Lifetimes of quantum well states and resonances in Pb overlayers on Cu(111)

A. Zugarramurdi,[1,2] N. Zabala,[1,2,3] V. M. Silkin,[2,3,4,5] A. G. Borisov,[6] and E. V. Chulkov[2,3,4]
[1]*Elektrizitatea eta Elektronika Saila, Zientzia eta Teknologia Fakultatea, UPV/EHU, 644 P.K., 48080 Bilbao, Spain*
[2]*Centro de Física de Materiales CFM, Centro Mixto CSIC-UPV/EHU, 20018 San Sebastián/Donostia, Spain*
[3]*Donostia International Physics Center (DIPC), P. de Manuel Lardizabal 4, 20018 San Sebastián/Donostia, Spain*
[4]*Departamento de Física de Materiales, Facultad de Ciencias Químicas, Universidad del País Vasco UPV/EHU, Apartado 1072, 20080 San Sebastián/Donostia, Spain*
[5]*IKERBASQUE, Basque Foundation for Science, 48011 Bilbao, Spain*
[6]*Laboratoire des Collisions Atomiques et Molèculaires (CNRS UMR 8625), Universitè Paris-Sud, Bâtiment 351, 91405 Orsay Cedex, France*

(Received 10 May 2009; revised manuscript received 17 August 2009; published 21 September 2009)

We present results of calculations of the lifetimes of excited electrons (holes) in quantum well states and quantum well resonances in Pb overlayers supported on Cu(111). Many-body decay via inelastic energy relaxation and one-electron decay via energy-conserving one-electron transfer into the substrate are considered. One-electron energies and wave functions have been computed for different coverages of the Pb overlayer (from 1 to 18 monolayers) by using a one-dimensional pseudopotential for the entire overlayer-substrate system in the framework of density functional theory within the local density approximation. The elastic (energy-conserving resonant electron transfer) contribution to the total lifetime broadening of quantum well resonances has been calculated within the wave packet propagation method. The inelastic electron-electron (many-body) contribution to the lifetime broadening of both occupied and unoccupied quantum well states has been evaluated using *GW* approximation. The decay mechanisms of both quantum well states and quantum well resonances in thick overlayers are discussed.

DOI: 10.1103/PhysRevB.80.115425 PACS number(s): 73.21.Fg, 73.50.Gr, 73.20.At, 78.47.−p

I. INTRODUCTION

Confinement of valence electrons in metallic films, as thin as a few electron Fermi wavelengths, results in discrete quantum well states (QWSs), which are the origin of quantum size effects in the properties of the system. In metallic overlayers adsorbed on metals or semiconductors the confinement is due to the vacuum barrier and the reflecting barrier at the interface caused by the energy gap in the substrate band structure projected onto the plane parallel to the interface. In the absence of a confining energy gap, another type of states of resonant character extending over the whole system, called quantum well resonances (QWRs), can exist.

Among various systems, the growth of Pb on Si(111) and Cu(111) has attracted much interest. Since the pioneer studies by Toennies and co-workers with He atom scattering,[1,2] different experimental techniques such as scanning tunneling microscopy[3,4] or surface x-ray diffraction have been used to probe the most stable heights of Pb islands on Cu(111) and Si(111) (Ref. 5) substrates. In favorable conditions, the islands cover wide areas forming overlayers of "magic" heights. The overlayer thickness can be crucial for the properties of the system, as for example the superconducting transition temperature.[6–10] The existence of magic heights with bilayer periodicity and the corresponding oscillations in the energetics of the overlayers as a function of the coverage have been studied theoretically using different approaches. Within density functional theory (DFT), first-principles[11] and jellium model[12] calculations for freestanding Pb films have been reported. In this context, a one-dimensional (1D) pseudopotential for the entire overlayer-substrate systems has been used to calculate the electronic structure of Pb/Cu(111) with different thicknesses of the Pb overlayer. This model has described well the electron confinement in the overlayers[13,14] and has given fairly good account of the experimental measurements of magic height distributions.[3]

Angle-resolved photoemission has been used to probe Pb thin films grown on different substrates.[15–17] In the photoemission spectra there are peaks which are considered as QWSs but appearing out of the projected gap of Cu(111). This confinement in the absence of a band gap has also been pointed out in other quantum well systems such as Al/Si(111), Pb/Si(111), and Na/Al(111).[18–20]

Most theoretical studies have focused on the electronic structure of these systems[21,22] and less attention has been paid to the study of the electronic excitations. Electronic excitations in metal surfaces play an important role in many chemical and physical phenomena.[23] They are characterized by their lifetime, which sets the duration of the excitation and, when combined with the group velocity, determines the mean free path, i.e., spatial range of the excitation. It was shown that on clean metal surfaces the decay of excited electrons and holes is closely related to dimensionality of the system, i.e., intraband transitions within the surface state band itself are mostly responsible for the final lifetime of the excited quasiparticle.[24,25] Even for a QWS in a 1 monolayer (ML) Na/Cu(111) the intraband transitions are crucial for the description of the hole decay in this state.[26] Recently, Kirchmann and Bovensiepen[27] used time-resolved two-photon photoemission technique, which allows the direct monitoring of the decay of excited electrons in the time domain,[28,29] to investigate the dynamics of QWSs in the Pb/Si(111) system as a function of the Pb thickness. They concluded that the intersubband decay in low-dimensional metallic systems is very important in order to interpret correctly experimental

results. They also suggested the Pb/Cu(111) system as a possible candidate to compare the decay of QWSs in Pb overlayers on different substrates. Hence theoretical study of the dynamics of the Pb/Cu(111) system would be very helpful for the understanding of future experiments on Pb overlayers.

Here we present the calculations of the lifetimes of excited electrons and holes in Pb overlayers on Cu(111) for different coverages. The electronic structure of the entire Pb/Cu(111) system is computed by using a 1D pseudopotential for the substrate-overlayer system, detailed elsewhere.[13,14] The contributions to the lifetime broadening are calculated using two approaches. The inelastic electron-electron (e-e) or many-body contribution to the lifetime broadening of both occupied and unoccupied quantum well states is evaluated using the *GW* approximation,[30] whereas the elastic (one-electron energy-conserving transfer through the Pb/Cu interface) contribution is calculated within the wave packet propagation (WPP) method. We leave for future studies and so do not address here the excited state decay via electron (hole)-phonon scattering as well as possible band folding effect because of the lattice mismatch between adsorbate and substrate.[31]

The paper is organized as follows. In Sec. II A we describe briefly the 1D model used to compute the electronic structure of the overlayer Pb/Cu(111) system. In Sec. II B, the many-body *GW* method is presented and in Sec. II C, the WPP one-electron method is outlined. In Sec. III, we present the obtained results and discussion. First, we develop some analytical expressions which are used in Secs. III A–III C dedicated to the lifetimes of QWSs and QWRs. Finally, in Sec. IV, the conclusions of the work are given. Unless stated otherwise, atomic units (a.u.) (i.e., $\hbar=e^2=m_e=1$) are used throughout the paper.

II. CALCULATION METHODS

A. General description

We have performed self-consistent electronic structure calculations for the Pb/Cu(111) overlayer-substrate system in the DFT framework[32] within a local density approximation (LDA)[33,34] and using the 1D model that was described in detail elsewhere.[14] Here we only give a brief description of the model. Basically we consider slabs characterized by translational invariance, i.e., a homogeneous free-electron gas, along the surface (*xy* plane). In this picture a single-particle wave function with two-dimensional (2D) wave vector $\mathbf{k}_\parallel$ parallel to the slab surface and quantum number j is represented in the form

$$\Psi_{j\mathbf{k}_\parallel}(\mathbf{r}) = e^{i\mathbf{k}_\parallel\cdot\mathbf{r}}\phi_j(z), \tag{1}$$

where $\phi_j(z)$ is the wave function in the direction perpendicular to the surface. The corresponding one-electron energies are then given by paraboloidal subbands,

$$E_{j\mathbf{k}_\parallel} = E_j + \frac{k_\parallel^2}{2m_j^\star}, \tag{2}$$

where E_j is the eigenvalue of the jth perpendicular state $\phi_j(z)$, corresponding to the minimum of the jth subband. The corrugation effects along the surface are reflected in effective masses $m_j^\star$ which can be included following Ref. 26. However, in the present work, we use $m_j^\star=1$ for all bands. Indeed, the main conclusions and results reported in this paper are robust with respect to the specific choice of the effective mass. Moreover, as far as we know, there are no published effective masses of QWSs for all energies in the Pb/Cu(111) system.

The energies E_j and wave functions $\phi_j(z)$ are obtained from the numerical solution of 1D Kohn-Sham equations with an effective or screened potential given by

$$V_{\text{eff}}(z) = 2\pi\int [\varrho_-(z') - \varrho_+(z')]|z-z'|dz' + V_{\text{xc}}[\varrho_-(z)] + V_{\text{ps}}(z), \tag{3}$$

where the first term on the right-hand side is the Hartree term, $V_{\text{H}}(z)$, which includes the electronic density $\varrho_-(z)$ and the neutralizing positive background $\varrho_+(z)$. The second term gives the LDA exchange-correlation potential and the third term accounts for the 1D pseudopotential. The overlayer-substrate system pseudopotential $V_{\text{ps}}(z)$ has two contributions, one from Pb and the other one from Cu(111).

For Cu(111) we construct 1D pseudopotential using the model potential proposed by Chulkov *et al.*[35] This model potential mimics the atomic structure of Cu(111) in the z direction, and it has been adjusted to correctly reproduce the experimental work function of Cu(111) of 4.94 eV, as well as the projected bulk band structure and the surface state at the $\bar{\Gamma}$ point.[35]

The free-electron-like character of electronic states at the Fermi level in lead[11,36] justifies the use of a stabilized jellium or the averaged pseudopotential[37,38] approach allowing us to simulate any Pb slab thickness. Then, the Pb slabs are described by the Pb density parameter, $r_s=2.30$ a.u., and a constant shift, $V_{\text{stab}}=-1.8$ eV, relative to the vacuum level, restricted to the region of the positive background charge and employed to stabilize the electron gas at the corresponding density. The stabilized jellium model used for description of the Pb films provides a proper work function so that the electron charge density spilling into vacuum is well described. Moreover, since the energy of the bottom of the valence electron band in bulk Pb is well reproduced, we obtain the correct Fermi wavelength λ_F and guarantee the proper description of the electron confinement and related properties.

The projected electronic structure of bulk Pb onto the (111) surface Brillouin zone contains a band gap between *s* and *p* electronic states that arises due to scalar relativistic effects.[11,36,39–41] The gap located between −8 and −4 eV with respect to the Fermi level is not taken into account in our model. Therefore, the results reported here for the QWSs falling into the corresponding energy range should be compared to the experimental data with caution. Nevertheless, we believe that the presentation of the results should not be limited to the states with energies well above the *L* gap of Pb. The discussion of all the confined states resulting from the jellium model for the overlayer is useful in the general context of the metal-overlayer/metal system.

Proceeding as described in Ref. 14, we finally obtain the 1D effective or screened potential for the entire system. With this potential, Kohn-Sham equations are solved in the z direction by discretization in a regular 1D mesh and using the Rayleigh quotient multigrid method.[42,43] In practice, our computational system is a Cu(111) slab of finite thickness, comprising 15–25 Cu(111) layers covered on both sides by the Pb overlayers. The symmetry and the finite size of the system in the DFT study lead to the symmetric effective potential V_{eff} and a discrete energy eigenvalue spectrum corresponding to the symmetric and antisymmetric states.

B. Inelastic contribution: Many-body *GW* method

The QWSs appear at the energies inside the projected band gap of Cu(111) or below the Cu(111) valence *sp* band. These states are stationary within the one-electron picture and correspond to an electron trapped in the quantum well formed by Pb overlayer. The QWSs decay via inelastic electron-electron scattering processes which can be described by many-body techniques. Below, we give a brief description of the many-body method, which we employ to calculate the inelastic electron-electron contribution to the lifetime broadening of occupied (holes) and unoccupied (excited electrons) QWSs. This formalism was used previously, for example, for the study of the quasiparticle dynamics on metal surfaces.[23,24,44,45] The inelastic linewidth, $\Gamma_{\text{e-e}}$ (or inverse lifetime, $\tau_{\text{e-e}}^{-1}$), of an electron or hole in the initial state Ψ with energy E is given by the projection of the imaginary part of the self-energy, Σ, onto this initial state,

$$\Gamma_{\text{e-e}} = \tau_{\text{e-e}}^{-1} = -2\int\int d\mathbf{r}d\mathbf{r}'\Psi^*(\mathbf{r})\,\text{Im}\,\Sigma(\mathbf{r},\mathbf{r}';E)\Psi(\mathbf{r}'). \tag{4}$$

The self-energy is computed in the *GW* approximation, which represents the first term in a series expansion of Σ in terms of the screened Coulomb interaction W. Then, the full one-electron Green's function G is replaced by the noninteracting Green's function G^0. For the present 1D effective potential, wave functions are in the form of Eq. (1) and the energies are expressed according to Eq. (2).

Substituting the wave functions and energies in Eq. (4) by those from Eqs. (1) and (2), the following equation for the decay rate of a quasiparticle with energy E_j and momentum $\mathbf{k}_\parallel$ (at the $\bar{\Gamma}$ point $\mathbf{k}_\parallel=0$) is obtained:

$$\Gamma_{\text{e-e}}^{j} = -2\int\int dzdz'\,\phi_j^*(z)\,\text{Im}\,\Sigma(z,z';\mathbf{k}_\parallel,E_j)\phi_j(z'), \tag{5}$$

where the 2D Fourier transform of the imaginary part of the self-energy Im Σ is given by

$$\text{Im}\,\Sigma(z,z';\mathbf{k}_\parallel,E_j) = \frac{1}{(2\pi)^2}\sum_{E_{j'}}^{0\le\pm(E_j-E_{j'})\le\pm(E_j-E_F)}\phi_{j'}^*(z')\phi_{j'}(z) \times\int \text{Im}\,W\left(z,z';\mathbf{k}_\parallel-\mathbf{q}_\parallel,\left|E_j-E_{j'}+\frac{\mathbf{k}_\parallel^2}{2}-\frac{\mathbf{q}_\parallel^2}{2}\right|\right)d\mathbf{q}_\parallel. \tag{6}$$

The upper limit in the sum over final states "+" ("−") stands for electrons (holes). The imaginary part of the screened interaction, Im W, satisfies the following integral equation:

$$\text{Im}\,W(z,z';\mathbf{q}_\parallel,E) = \int\int dz_1dz_2V(z,z_1;\mathbf{q}_\parallel) \times \text{Im}\,\chi(z_1,z_2;\mathbf{q}_\parallel,E)V(z_2,z';\mathbf{q}_\parallel). \tag{7}$$

Here $V(z,z';\mathbf{q}_\parallel)$ and $\chi(z,z';\mathbf{q}_\parallel,E)$ are the 2D transforms of the bare Coulomb interaction and the density response function of the interacting electron system, respectively. Within the random phase approximation (RPA), $\chi(z,z';\mathbf{q}_\parallel,E)$ obeys the integral equation,

$$\chi(z,z';\mathbf{q}_\parallel,E) = \chi^0(z,z';\mathbf{q}_\parallel,E) + \int\int dz_1dz_2\chi^0(z,z_1;\mathbf{q}_\parallel,E) \times V(z_1,z_2;\mathbf{q}_\parallel)\chi(z_2,z';\mathbf{q}_\parallel,E). \tag{8}$$

χ^0 is the density response function for the noninteracting electron system. It can be calculated in terms of both eigenfunctions $\phi_j(z)$ and eigenvalues E_j of the 1D model potential. We use the expression derived by Eguiluz[46] for χ^0, assuming free-electron motion ($m_j^*=1$ for all j) in the plane parallel to the surface.[47] With these effective masses, our calculations of χ^0 take explicitly into account all band structure effects in the direction perpendicular to the surface.

C. Elastic contribution to the decay of quantum well resonances

The QWRs appear at the energies outside the projected band gap of Cu(111) and correspond to the electrons transiently localized in the Pb overlayer because of the finite reflectivity of the Pb/Cu(111) interface. Along with possible many-body decay, QWRs decay via energy-conserving (resonant) one-electron transfer into the bulk continuum of Cu(111). These quasistationary states (resonances) thus correspond to the Lorentzian peaks in the electronic density of states (DOS), where the energies of the resonances and their one-electron decay rates are associated with the energies E and widths Γ_{res} of the peaks.

For the calculation of the energies and one-electron decay rates of the QWRs, we use the 1D WPP approach detailed elsewhere.[48–51] The method consists of the direct solution of the time-dependent 1D Schrödinger equation for the wave function $\phi(z,t)$ of the "active" electron,

$$i\frac{\partial\phi(z,t)}{\partial t} = H(t)\,\phi(z,t), \tag{9}$$

subjected to the initial conditions, $\phi_0\equiv\phi(z,t=0)$. $H=-\frac{1}{2}(\partial^2/\partial z^2)+V(z)+V_{\text{abs}}(z)$ is the Hamiltonian of the system. The potential $V(z)$ is constructed on the basis of the effective potential $V_{\text{eff}}(z)$ calculated within DFT (see Sec. II A) in such a way that it describes the Pb overlayer deposited on the semi-infinite Cu(111) substrate. The spurious effects due to the quantization of the continuum states in the supercell geometry are removed. In practice, $V(z)=V_{\text{eff}}(z)$ in the surface region containing the Pb overlayer. Starting from approximately fifth Cu atomic layer and further into the bulk, the

overlayer appears completely screened. The model potential[35] describing electron interaction with Cu(111) is then used for $V(z)$ with vacuum level set in such a way that the actual work function change is taken into account. $V_{\text{abs}}(z)$ is the absorbing potential introduced at the grid boundaries in order to suppress the artificial reflections of the wave packet and guarantee the outgoing wave boundary conditions consistent with the quest for the quasistationary states. The calculation mesh comprises $N_z=8192$ points with grid spacing $\Delta z=0.2$ a.u. The time propagation step is $\Delta t=0.05$ a.u. and the typical calculation takes 4×10^5 time steps.

From $\phi(z,t)$, the survival amplitude or the autocorrelation function of the initial wave packet $A(t)=\langle\phi_0|\phi(t)\rangle$ can be derived. The real part of the time-to-energy Laplace transform of $A(t)$ gives $\eta(\omega)$, the energy-resolved density of states projected onto the initial state (PDOS),

$$\eta(\omega)=\mathrm{Re}\left(\lim_{\epsilon\to0^+}\frac{1}{\pi}\int_0^T e^{i(\omega+i\epsilon)t}A(t)dt\right), \tag{10}$$

where T stands for the large but finite calculation time. The PDOS $\eta(\omega)$ is then used to extract the energies and widths of the QWRs. It is noteworthy that the stationary within one-electron picture QWSs appear in $\eta(\omega)$ as sharp peaks with the widths $\Gamma\sim1/T$. Thus, the energies of the QWSs can be extracted from the WPP approach in parallel to the DFT calculations allowing consistency checks.

The appropriate choice of the initial state ϕ_0 can strongly ease the extraction of the energies and widths of the QWRs. Indeed, the main contribution to the PDOS comes from the quantum well localized states strongly overlapping with ϕ_0. We used the initial sharp Gaussian wave packet centered at the vacuum-overlayer interface. In this region the QWSs show similar behavior with exponential decay into the vacuum. Thus, they have similar overlap with the initial state.

An example of the calculated PDOS is shown in Fig. 1 for the case of 6 ML of Pb on Cu(111). The energy range spanned in the figure corresponds to the one between the bottom of the Cu(111) valence *sp* band and the onset of the projected band gap (*L* gap) of Cu(111). In this energy range the quantum well localized electronic states can decay via energy-conserving electron transfer into the substrate so that QWRs are formed. These appear as Lorentzian peaks in PDOS labeled by their principal quantum number. Observe that the width of the resonance decreases as its energy approaches the bottom of the Cu(111) *sp* band or of the projected band gap (*L* gap). This can be explained as the increase in the reflectivity of the Pb/Cu(111) interface leading to the stabilization of the QWRs. The detailed account of the results and the discussion of the energies and decay rates of the Pb overlayer states is presented in Sec. III.

III. RESULTS AND DISCUSSION

A. Energies of the QWSs and QWRs

We start our discussion from some general considerations allowing transparent analysis of the numerical results. Assume the Pb overlayer at Cu(111) with an effective width d.

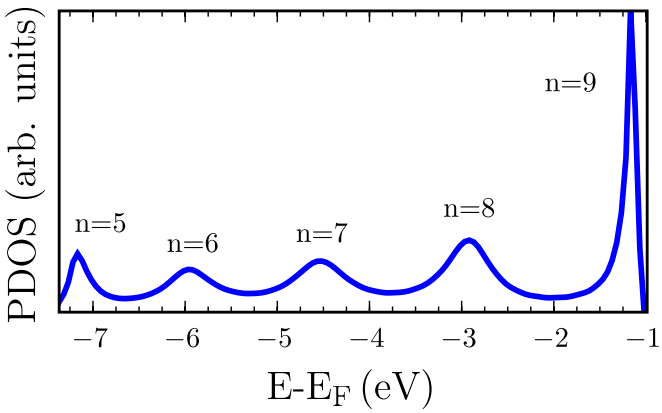

FIG. 1. (Color online) PDOS at the $\bar{\Gamma}$ point for 6 ML of Pb on a Cu(111) surface. Free-electron model for the Pb overlayer is used. Results are shown as a function of the energy measured with respect to the Fermi level. The QWRs are labeled according to their principal quantum number n (see discussion in Sec. III A). The energy range spans an interval between the bottom of the Cu(111) valence band and the bottom of the Cu(111) *L* gap, where the states localized in the Pb overlayer can decay via one-electron tunneling into the substrate.

Here d is not simply given by the number of the Pb MLs but effectively accounts for the scattering properties of the Pb/vacuum and Pb/Cu(111) interfaces. An example of the one-electron potential for such a system is shown in Fig. 2(a) for the case of the 6-ML-thick Pb overlayer.

For a freestanding Pb overlayer of the thickness d one expects a series of quantized states at $\bar{\Gamma}$ with energies $E_n\simeq0.5(n\pi/d)^2$ as measured with respect to the bottom of the potential well. For the supported overlayer, one of the Pb/vacuum interfaces of the freestanding film is replaced by the Pb/Cu(111) interface so that different types of states are formed depending on their energy E_n with respect to the projected band structure of Cu(111).

(i) E_n is in energy resonance with propagating electronic states inside the Cu(111) [white energy region in Fig. 2(a)]. In this case, the electron initially localized in the overlayer quantum well can be transferred into the Cu(111) substrate. The corresponding overlayer state becomes quasistationary with the width given by the rate of the energy-conserving (resonant) electron transfer into the substrate Γ_{res}. We refer to these states as QWRs.

(ii) E_n is in the projected band gap of Cu(111) [top colored (blue) energy region in Fig. 2(a)]. The resonant electron transfer from the jellium Pb overlayer into the Cu substrate is then impossible. The overlayer localized states are stationary in a one-electron sense, and the only possible decay channel is due to the many-body interactions. These are the gap QWSs or g-QWSs.

(iii) E_n is below the bottom of the Cu(111) *sp* band; the resonant electron transfer into the Cu substrate is impossible similar to the situation described in (ii). The corresponding energy range is the bottom colored region (green) in Fig. 2(a), with the difference of ($\approx$2 eV) between the average Cu(111) and Pb potentials. In this work we use notation deep QWSs (d-QWSs) for the states existing in this energy region to distinguish them from the g-QWSs.

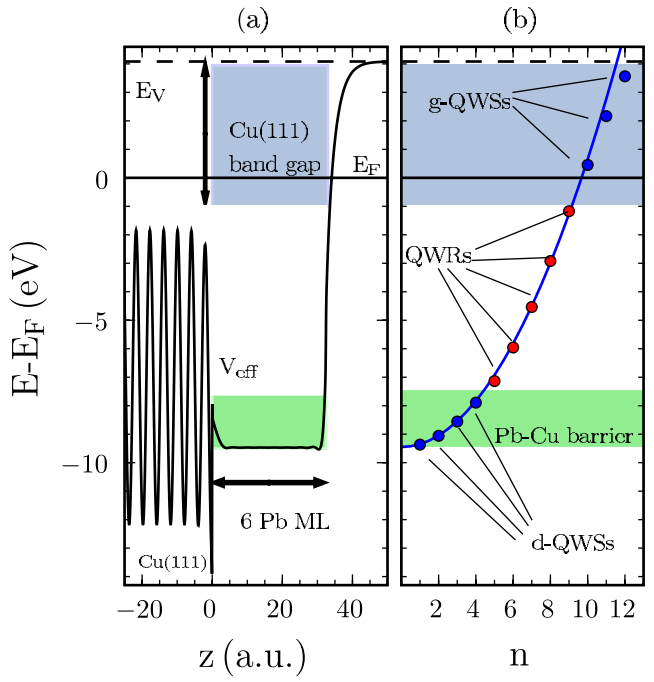

FIG. 2. (Color online) (a) Effective potential V_{eff} (solid line) for 6 ML of Pb on a Cu(111) surface. The origin $z=0$ is situated at one half of the Cu(111) interlayer spacing from the Cu surface layer (it coincides with the Pb jellium edge). The energies are given with respect to the Fermi level, E_F. The horizontal dashed line represents the vacuum level. The energy regions where QWSs localized in Pb overlayer can exist are shaded with colors. The top colored region (blue) corresponds to the projected Cu(111) band gap and the bottom colored region (green) corresponds to the differences in average potentials in Pb and Cu(111). In between these two energy regions the overlayer localized states are in resonance with bulk propagating states of the substrate so that QWRs are formed. (b) Energy eigenvalues as a function of their quantum number n. Dots (blue) in colored regions are localized QWSs and (red) dots in white region represent QWRs. The parabola (continuous blue line) is plotted as reference.

In Fig. 2(b), the energies of the QWSs and QWRs are plotted for $k_{\parallel}=0$ as a function of their quantum number n for the 6 ML Pb/Cu(111). The energies of the QWSs correspond to the eigenvalues of the effective 1D Hamiltonian as calculated within DFT approach. The energies of the QWRs were obtained from the positions of the peaks in PDOS as calculated with WPP (see Fig. 1). The quantum number of the state n can be assigned through the nodal structure of the corresponding wave function inside the Pb overlayer. In Fig. 3 the electronic densities of the QWSs and QWRs are shown for the 6 ML Pb/Cu(111) system. Despite different behaviors inside the metal—exponentially decaying bound state for QWSs and propagating state for QWRs—the number of nodes inside the Pb overlayer forms a continuous sequence with increasing energy of the states. This reflects the common origin of the QWSs and QWRs as the states confined in the Pb overlayer due to the reflectivity of the Pb/Cu(111) interface. Thus, the energies of the states irrespective of their stationary or quasistationary character can be well described with single parabolic fit,

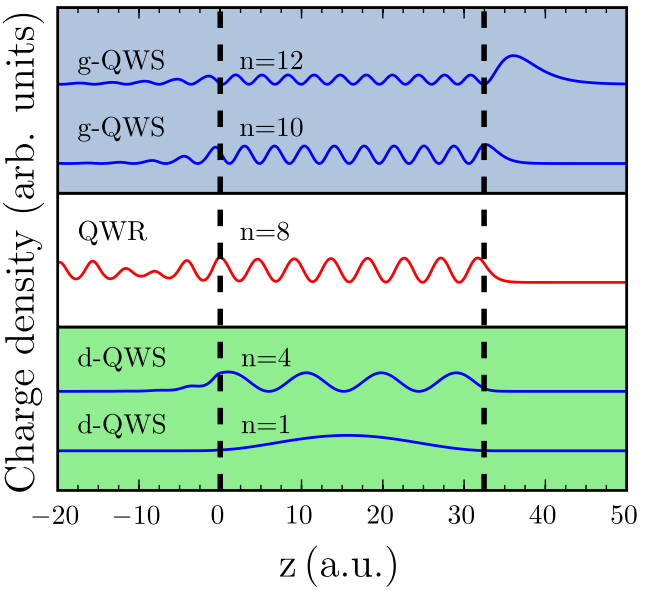

FIG. 3. (Color online) Charge density of some QWSs (blue lines in colored regions) and QWRs (red line in white region) for the 6 ML Pb/Cu(111) system. Results are shown as a function of the z coordinate perpendicular to the surface. For the definition of the z axis and shaded regions see caption to Fig. 2. The states are labeled according to their n quantum number reflecting the nodal structure inside the Pb potential well. Vertical dashed lines delimit the Pb overlayer region.

$$E_n = 0.5(n\pi/d)^2 \sim (n/J)^2, \tag{11}$$

where d stands for the effective thickness of the overlayer and J is the number of MLs. However, it should be noted that despite common energetics there is an essential difference between QWSs and QWRs: for the former the reflectivity of the Pb/Cu barrier $\mathcal{R}=1$ and for the latter $\mathcal{R}<1$ allowing one-electron decay via tunneling into the bulk.

In Fig. 4 the calculated energies of the gap QWSs (black dots) and QWRs (red dots, in bottom region below ~ -1 eV) are shown as a function of the overlayer thickness for Pb/Cu(111). Present results are compared with angle-resolved photoemission experimental data[15] shown with triangles. The agreement between calculated and measured energies of the QWSs and QWRs is noteworthy. This gives a confidence in the modeling of the overlayer/substrate system. Indeed, the calculations match the experimental data even for Pb coverages as low as 3 ML, where the jellium description of Pb overlayer could be questioned. For the state with a given quantum number, the calculated energies show the $1/J^2$ dependence with Pb overlayer thickness in full agreement with Eq. (11). Experimentally, assignation of the given quantum number to an observed feature and following the change in the energy of this state are not trivial tasks.[14] Therefore, for the connection between theoretical results and an experiment the way the experimental data are analyzed is of central importance. In a number of experimental studies, appearance of the states within certain energy intervals has been addressed, as has been done in scanning tunneling spectroscopy study of the Pb overlayers on Cu(111).[52] One char-

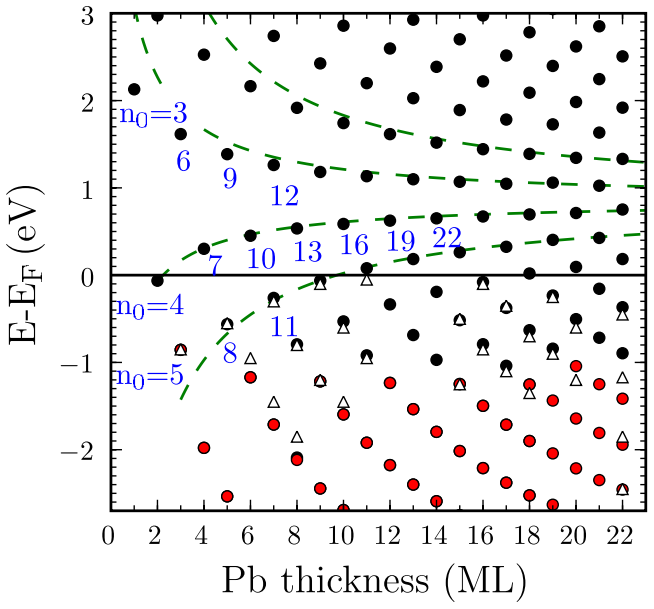

FIG. 4. (Color online) Calculated energies of the gap QWSs (black dots) and QWRs (red dots, in bottom region below ~−1 eV) for Pb overlayers on Cu(111). Results are shown as a function of the overlayer thickness. Angle-resolved photoemission experimental data (Ref. 15) (triangles) are plotted for comparison. Dashed lines connecting the states are the closest-energy lines calculated with Eq. (12). Some states are marked with the corresponding n quantum numbers. n_0 are the initial quantum numbers which label the lines. The energies are given with respect to the Fermi level (horizontal line).

acteristic feature of those experimental results was observation of QWSs at 0.65 eV above E_F for an even number of MLs. In our DFT calculations, shown in Fig. 4, we also find that for an even number of MLs, above the 6 MLs coverage, there is systematically a state with an energy close to 0.65 eV. However, it is important to realize that the quantum number n of this state changes with changing coverage.

In Fig. 4 we show "closest-energy lines" which connect the closest in energy QWSs near the Fermi level and for variable Pb overlayer thickness. In what follows, we present a simple analytical description of these closest-energy lines. It appears useful in the discussion of experimental results in that it allows an assignment of the quantum numbers for the states appearing close in energy for increasing coverage. We start from the observation that for the calculated states close to the Fermi level, which are at about 9.5 eV above the bottom of the overlayer confining potential, the quantum number n increases by approximately three units every 2 ML of Pb (the thickness of a Pb ML is taken $a=5.41$ a.u.). Then, the closest-energy lines can be derived from this observation and Eq. (11) as follows:

$$E_{n_0,d_0,\Delta J} = \frac{\pi^2}{2}\left[\frac{n_0 + \frac{3}{2}(J-J_0)}{d_0 + a(J-J_0)}\right]^2, \tag{12}$$

where n_0 and d_0 are some initial quantum number and corresponding effective thickness that label the given line and J_0 corresponds to the initial number of MLs from which the closest-energy line is traced. $\Delta J = J - J_0$ is the change in the coverage as measured in number of MLs, $n_{n_0,\Delta J} = n_0 + \frac{3}{2}(J - J_0)$ is an "effective" continuous quantum number of the states along the line, and $d = d_0 + a(J - J_0)$ is an effective thickness. This effective thickness is also expressed as $d = Ja + \delta$, where δ is the width associated to the electron charge spilling, which can be either considered as a free parameter or it can be obtained from DFT calculations and using the phase accumulation model[53] to evaluate the phase shifts for the confinement barriers, as it was done by Ogando *et al.*[14] Notice that δ varies with the energy of the state. However, a constant value of $\delta = 4.2$ a.u. fits the energy of calculated states around the Fermi level.

Using the relation $J - J_0 = (d - d_0)/a$ the energy can also be defined as a function of the total width d,

$$E_{n_0,d_0} = \frac{\pi^2}{2d^2}\left[n_0 + \frac{3}{2a}(d - d_0)\right]^2. \tag{13}$$

With $n_0 = 3, 4, 5$ and the corresponding d_0 effective thickness this equation provides fairly good description of the closest-energy lines shown in Fig. 4. For the thick overlayers, such that $d \gg d_0$, Eq. (13) leads to the following asymptotic expansion:

$$E - E_F = \alpha/d + \beta,$$

$$\alpha = \frac{3\pi^2}{2a}\left(n_0 - \frac{3}{2}\frac{d_0}{a}\right),$$

$$\beta = \frac{9\pi^2}{8a^2} - E_F. \tag{14}$$

Thus, e.g., observing the photoemission peaks for thick layers one would have an impression that QWSs basically do not change their energy with increasing thickness and periodicity of 2 ML. However, this has to be taken with caution since the underlying quantum number of the QWSs does change.

B. Decay of quantum well states

We have performed *GW* calculations of the lifetime broadening at the $\bar{\Gamma}$ point for the QWSs in Pb overlayers of thicknesses ranging from 1 to 18 ML. Some results are shown in Table I. The calculated electron-electron inelastic decay rates of d-QWSs are in the range of 1–2 eV which places their lifetimes in the fraction of the fs range. This is an evident consequence of the deep energy position of these states so that the large phase space is available for the many-body energy relaxation process. On the other hand, depending on the overlayer thickness, the g-QWSs can *a priori* appear at energies close to the Fermi level.

In Fig. 5 we present the calculated many-body decay rates $\Gamma_{e\text{-}e}$ of the g-QWSs as a function of their energy measured with respect to the Fermi level. Results are shown up to the QWS energy of 3 eV only. For states with higher energies the image potential tail of the electron-surface interaction be-

TABLE I. Calculated energy, E, linewidth, Γ, inverse decay rate, Γ^{-1}, and corresponding quantum number, n, of some QWSs (many-body decay) and QWRs (resonant decay) calculated for selected Pb overlayer thicknesses.

No. of MLs	$E-E_F$ (eV)	Γ (meV)	Γ^{-1} (fs)	n
6[a]	−1.17	161	4	9
6	0.45	2	289	10
6	2.16	68	10	11
8	−2.12	380	2	11
8	−0.79	18	36	12
8	0.53	4	177	13
8	1.92	55	12	14
9	−2.44	411	2	12
9[a]	−1.22	117	6	13
9	−0.06	Small	High	14
9	1.18	26	26	15
9	2.43	85	8	16
10	−2.69	377	2	13
10	−1.60	210	3	14
10	−0.53	8	83	15
10	0.59	5	121	16
10	1.74	48	14	17
10	2.86	103	6	18
18	−2.53	194	3	23
18	−1.91	162	4	24
18	−1.26	74	9	25
18	−0.64	10	70	26
18	0.01	Small	High	27
18	0.69	10	69	28
18	1.38	34	19	29
18	2.08	69	10	30
18	2.78	108	6	31

[a]Result has to be taken with caution because the calculated peak overlaps with the energy gap region.

comes important[53–55] and it is not well described within present DFT treatment. The computed decay rates are compared with that for excited electrons and holes in a homogeneous electron gas obtained from the Quinn-Ferrell (QF) formula.[56] The QF expression describes the decay rate Γ_{QF} in the high electron density limit for states with energies close to the Fermi level, E_F,

$$\Gamma_{QF} = \hbar\tau_{QF}^{-1} \approx 2.5019 r_s^{5/2}(E-E_F)^2. \quad (15)$$

In this equation τ_{QF} is the lifetime of the excited state, the energy is in eV, and the decay rate, Γ_{QF}, is given in meV. We use the density parameter r_s corresponding to bulk Pb, i.e., r_s=2.3 a.u. As is seen in the figure, the calculated many-

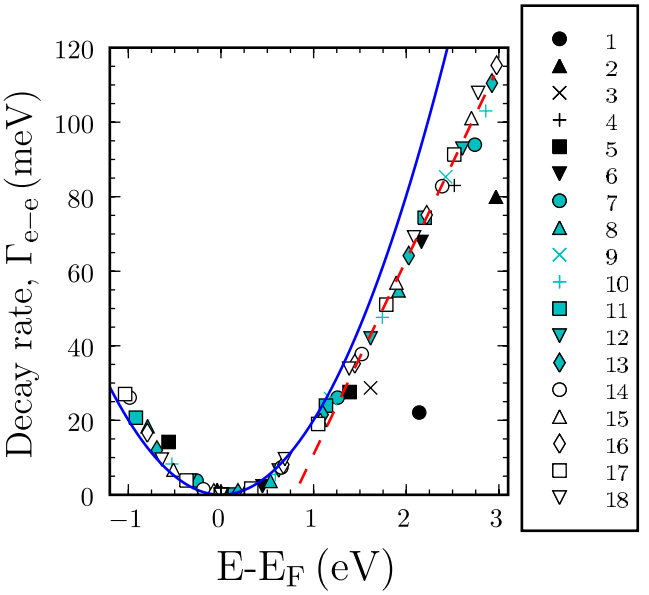

FIG. 5. (Color online) Calculated inelastic e-e decay rates (denoted by different symbols and colors) of QWSs laying in the gap energy region of the Pb/Cu(111) system. Results for the Pb overlayers from 1 to 18 ML thick are shown as a function of the energy measured with respect to the Fermi level of the corresponding system. The QF curve (continuous line) for the density of bulk Pb (r_s=2.3 a.u.) and a linear fit (dashed line) are plotted for reference.

body decay rate of states close to the Fermi level closely follows quadratic dependence given by Eq. (15). For the states with higher energies, from 1 up to 3 eV, a quasilinear dependence of the calculated $\Gamma_{e\text{-}e}$ on energy is observed signaling about deviation of the RPA linewidth from simple quadratic dependence.[57] This is further illustrated by the straight line with a slope of ≈52 meV eV^{-1} that fits the evaluated decay rate for the states between 1.3 and 3 eV and thicknesses above 6 ML. This quasilinear dependence can be attributed to the use of RPA in the description of the screening which does not give a quadratic dependence of the decay rate for relatively high energies.

For the Pb overlayers with small thickness (1–3 ML), the QWSs with energies above 1 eV have many-body decay rates well below the general trend obtained for thick overlayers. This can be understood from the relative weight of the wave function of the corresponding states in the vacuum and inside the film. For small binding energies the wave function of the state spreads more into the vacuum so that, for the thin overlayers, the probability to find an electron inside the overlayer reduces, leading to the reduction in $\Gamma_{e\text{-}e}$. The absence of the data points in the energy region between 0.7 and 1 eV is consistent with the overlayer thickness dependence of the energies plotted in Fig. 4. Note that this energy region corresponds to the change from the "nearest-energy line" with the positive slope (n_0=4) to that with the negative one (n_0=3).

Detailed analysis of the contribution of the different decay channels into the many-body decay rate of the g-QWSs is presented in Fig. 6 as a function of the Pb overlayer thickness. The states are along the n_0=5 closest-energy line as

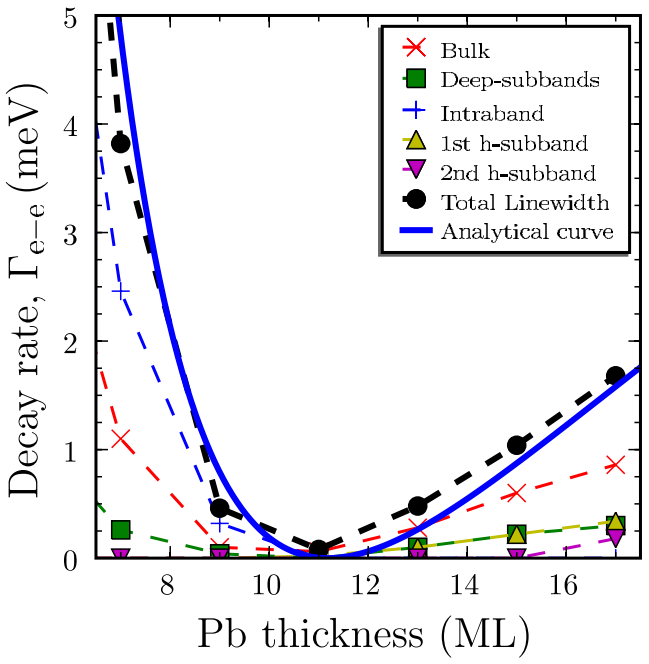

FIG. 6. (Color online) Linewidths and contributions of different decay channels in many-body decay of the QWSs located throughout the $n_0=5$ line in Fig. 4. Different decay processes are related to first and second highest subbands (h-subbands), deep QWS subbands, and, for occupied states, the intraband process. The solid line corresponds to the analytic formula in Eq. (16) with $r_s=2.3$ a.u. and width increase $\delta=4.2$ a.u.

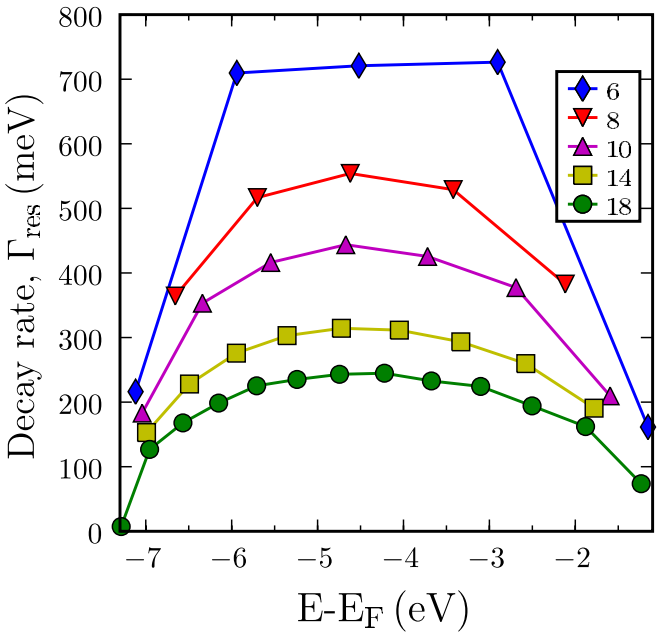

FIG. 7. (Color online) Calculated one-electron decay rates of QWRs for the jellium Pb overlayers on Cu(111). Results are shown as a function of the energy measured with respect to the Fermi level. Different symbols stand for the different overlayer thicknesses measured in Pb MLs as indicated in the insert of the figure.

appears in Fig. 4. As was discussed in Sec. III A this way of the data analysis is consistent with that often used experimentally, i.e., one traces the overlayer thickness dependence of the given property of the QWSs that appear closest in energy. Moreover, choice of this sequence of the QWSs allows us to follow the energy evolution from below to above the Fermi level.

From Fig. 6 one can conclude that even though the g-QWSs and the d-QWSs are well localized in the overlayer so that their overlap is large, the inelastic electron or hole transfer into the d-QWSs is small. This is because the d-QWSs have large binding energy at the $\bar{\Gamma}$ point so that the decay of an excited electron or hole from the g-QWS to the d-QWSs is accompanied by a large momentum transfer. This renders the process inefficient. The hole relaxation is associated with mostly intraband transitions and the bulk contribution is nearly three times smaller than the intraband one. This is similar to the results reported for the surface states.[24] As far as the excited electron is concerned, the intraband transitions are impossible from the $\bar{\Gamma}$ point. Transitions into the substrate bulk bands contribute then one half of the total decay rate. Another half of the decay rate comes from the interband scattering between QWSs.

Now we discuss briefly the total e-e decay rate of the QWSs as a function of the Pb coverage. Substituting the energies of the QWSs in Pb/Cu(111) system as given by Eq. (14) into the QF formula given by Eq. (15) leads to

$$\Gamma_{\text{e-e}} \approx 68.08 r_s^{5/2} \frac{(\alpha+\beta d)^2}{d^2}. \tag{16}$$

This result for the inelastic e-e decay rate of the QWSs close to the Fermi level is shown by the solid line (labeled "analytical curve") in Fig. 6. The good agreement between the numerical data and the analytical prediction is not surprising in view of the parabolic dependence of the calculated decay rate with energy close to E_F (see Fig. 5).

Finally we discuss the sensitivity of the calculated lifetimes to the choice of the effective mass. As we have stated in the section devoted to the theoretical methods, $m_n^*=1$ has been used in this study. In the experimental study in Ref. 15, effective masses ranging from 1.1 to 1.6 were reported for occupied QWSs. In order to estimate a possible effect, we have repeated calculations ascribing effective mass of 1.6 to the occupied QWS of 18 ML system and observed a slight increase in linewidths of order of 5–15 %. It means that presented results are rather robust to effective mass differences. In any case, we expect that corrections coming from a more elaborated modeling of the overlayer might be more important.

C. Decay of quantum well resonances

The calculated one-electron resonant decay rates Γ_{res} of QWRs are shown in Fig. 7. Results are presented as a function of the energy of the quasistationary states measured with respect to the Fermi level. For the given overlayer thickness, Γ_{res} is smallest for the lowest energy states energetically close to the bottom of the substrate valence band and for the highest energy states close to the onset of the Cu(111) L gap.

As we have already stated in connection with Fig. 1, this result can be explained by the high reflectivity of the substrate in the corresponding energy regions.[58] Indeed, in the quasiclassical picture an electron localized in the QWR of the Pb overlayer is moving back and forth in the quantum well hitting the Pb/vacuum and Pb/Cu interfaces. The decay rate can be then estimated from the simple expression,

$$\Gamma_{\mathrm{res}} = (1-\mathcal{R})\Delta E = (1-\mathcal{R})\pi\sqrt{E}/d, \tag{17}$$

where $\nu=\Delta E$ is the attempt (revival) frequency at which an electron is hitting the Pb/Cu interface. ΔE is the energy difference between the levels in the electron energy range of interest and $\mathcal{R}$ is the reflection probability of the Pb/Cu interface. Thus, when $\mathcal{R}\rightarrow 1$ the decay rate Γ_{res} tends to zero. There is another important conclusion from Eq. (17). From the energy quantization of the QWRs we obtain that $\Delta E = \pi\sqrt{E}/d$. Then, for the fixed energy interval the resonant decay rate decreases as $1/d$ with increasing thickness d of the Pb overlayer. This is fully supported by present numerical results shown in Fig. 7. Essentially the same conclusions follow from the more refined analytical treatment of the properties of the QWRs as reported in Ref. 59. Intuitively, the resonances become narrower, but their density increases so that in the limit of large d the continuum of Pb states is retrieved (see also Fig. 1).

It is noteworthy that in some cases the resonant peaks in the PDOS appear very close to the Cu(111) band gap so that Lorentzian resonant shape is distorted. Then, the decay rate was estimated from the low energy part of the peak. However, this result has to be taken with caution since non-Lorentzian shape of the PDOS reveals nonexponential decay. In Table I these QWRs are marked explicitly.

Along with resonant one-electron transfer through the Pb/Cu interface, the QWRs can decay by many-body processes, so that their total lifetime broadening depends on both decay channels. The exact calculation of the many-body decay of the QWRs is a nontrivial task and it was not attempted in the present study. Indeed, as has been shown in Ref. 60 the Γ_{res} and $\Gamma_{\mathrm{e\text{-}e}}$ may not contribute to the total decay rate of the resonances at surfaces in an additive way. Consider the bulk many-body contribution. The inelastic collisions with bulk electrons are most efficient inside the substrate. But when an electron enters the Cu(111), it is already lost from the point of view of the population of the Pb overlayer localized state. Thus, the resonance decay is mostly not affected by the many-body energy relaxation in the bulk. The latter process determines the population of the final states in the system, but not the decay rate of the QWRs.[60] On the other hand, the intraband transitions and interband transitions into the lower energy QWRs and QWSs should contribute to the population decay. With help of Fig. 6, we estimate that nonbulk transitions are responsible for approximately 60% of the many-body decay of the QWRs energetically located below the Fermi level. Thus, the QF curve with $r_s=2.3$ a.u. (see Fig. 5) should give a reasonable upper bound for the possible many-body contribution to the lifetime broadening of the QWRs.

Figure 8 is aimed at the qualitative discussion of the general trends determining the lifetimes of the QWRs. It shows

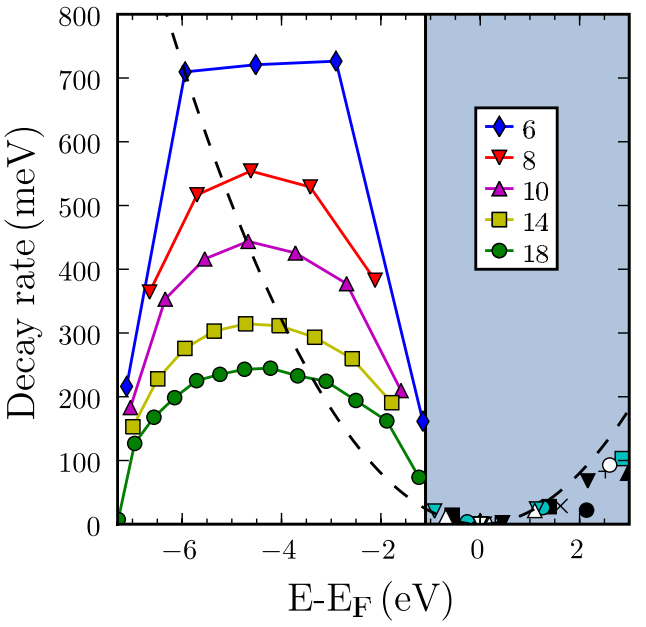

FIG. 8. (Color online) Calculated many-body (inelastic) decay rates of the QWSs and resonant (elastic) decay rates of the QWRs as a function of the energy measured with respect to the Fermi level. The shaded energy region corresponds to the projected band gap of the Cu(111) surface where the QWSs exist. The states appearing below the projected band gap are the QWRs. For the QWRs different symbols correspond to the overlayer thickness (see the inset). For the QWS the symbols are the same as in Fig. 5. Parabolic QF curve with Pb charge density parameter $r_s=2.3$ a.u. is shown by the dashed line.

the calculated many-body and one-electron decay rates of the QWSs and QWRs. The QF curve with $r_s=2.3$ a.u. allows extrapolation of the parabolic energy dependence of the inelastic decay rate of the QWSs into the energy region of the QWRs. As follows from the comparison between the calculated resonant decay rates and the QF estimation of the many-body decay, the latter will be the dominating decay channel for the low energy QWRs below −6 eV. For the QWRs at higher energies and near the projected band gap, the dominating decay mechanism will strongly depend on the overlayer thickness d. For thin layers, the resonant one-electron decay should dominate. However, since the resonant decay rate decreases as $1/d$, we estimate that for the overlayers of thickness above 30 ML the inelastic many-body scattering will be the dominating decay channel of the QWRs. This appears physically sound since for the thick Pb films the QWRs merge and form Pb bulk continuum of the electronic states where only many-body decay is operative.

In the angle-resolved photoemission study of thin Pb films on Cu(111) carried out by Dil *et al.*,[15] the states below the projected band gap of Cu(111) were observed along with conventional QWSs with energies inside the projected band gap of copper. In Ref. 15 these states were not associated with QWRs because their linewidths appeared comparable to that of the QWSs, i.e., without noticeable effect of the resonant charge transfer broadening. Based on the results of the present study we argue that for the thick Pb overlayers on

Cu(111) the QWRs appearing close to the projected band gap indeed show the linewidth comparable to that of the QWSs. It is noteworthy that the energies of the QWRs calculated with the present model for thick layers and experimental observations in Ref. 15, compared in Fig. 4, are in good agreement.

IV. SUMMARY AND CONCLUSIONS

We have calculated the lifetimes of QWSs and QWRs in Pb overlayers (up to 18 ML) supported on a Cu(111) substrate. The system is modeled with self-consistent 1D pseudopotential obtained from the density functional theory calculations with proper account for the projected band gap structure of the Cu(111) substrate and free-electron (jellium) representation of the Pb overlayer. This model has described very well the electron confinement in this system, in particular the energies of the QWSs.[13,14] It also has given fairly good account of the experimental measurements of magic overlayer height distributions.[3] On the qualitative level the results of the present study are representative for the free-electron-like metal overlayers on the substrates possessing the projected band gap.

For QWSs, the inelastic electron-electron contribution to the broadening has been calculated within many-body theory using the *GW* approximation. Our results show that d-QWSs located below −8 eV with respect to the Fermi level, i.e., below the bottom of the Cu(111) *sp* band, have many-body decay rates larger than 1 eV. Taking into account the small energy separation, the corresponding peaks in, e.g., photoemission spectra should completely overlap rendering impossible resolution of the individual states.

The QWSs laying in the projected energy gap of Cu(111) have much longer lifetimes. At small energies with respect to the Fermi level we find that the many-body decay rate approximately follows the QF parabolic dependence with energy. For the QWSs located at higher excitation energies a quasilinear dependence of the many-body decay rate with energy is found. As a general trend, we have found that the contribution of the Cu(111) bulk into the many-body decay of the overlayer localized states is comparable to that of the interband and intraband transitions involving directly QWSs.

QWRs appear energetically below the projected band gap of the substrate inside the Cu(111) *sp* band. Thus, an electron initially localized in the quantum well can escape into the substrate via energy-conserving tunneling through the Pb/Cu(111) interface. The one-electron elastic decay rates of the QWRs were calculated with WPP method for variable thickness of the overlayer revealing several general trends:

(i) The one-electron decay rate of the QWRs is small whenever the reflectivity of the Pb/Cu(111) interface is high, in particular close to the onset of the Cu(111) projected band gap. In this energy region the QWRs can have the widths comparable to that of the QWSs.

(ii) When the width d of the Pb overlayer increases, the decay rate of the QWRs decreases in overall as $1/d$. This can be understood on the basis of the simple quasiclassical arguments developed in the main text of the paper.

(iii) Comparing elastic decay rate of the QWRs with their many-body decay rate estimated from the QF formula, we conclude that for the overlayers thicker than 30 ML the inelastic decay will dominate. Basically this sets the transition to the limit of the thick Pb film, where only inelastic decay will be possible.

For the connection between theoretical results and experiment the issue of the way the experimental data are analyzed appears of central importance. Since experimentally the assignation of the given quantum number is not a trivial task, one can follow the energy evolution of the states with increasing overlayer thickness focusing at the given energy intervals. For the QWSs near the Fermi level which are explored in (two-photon) photoemission and scanning tunneling spectroscopy experiments, we have derived an analytical expression for the lifetime and energy evolution with the overlayer thickness.

Some comments are in order with respect to the possible effect of the projected band gap of Pb(111) overlayer. From the *ab initio* studies of the Pb(111) films and Pb(111) surface,[11,36,40,41] the L gap of the overlayer should be located between −8 and −4 eV with respect to the Fermi level of the system. Outside the Pb(111) L gap the parabolic dispersion is retrieved. Therefore, the main difference between the free-electron-like representation of the Pb overlayer and the realistic case will concern the QWRs with energies falling into the Pb L-gap region. They will be pushed to the extremities of the Pb L gap so that the energies and the decay rates obtained here with free-electron model will be modified. As to the QWRs located above −3 eV, we expect that the results reported here will hold. Currently a study including the projected band gap of the Pb(111) overlayer as well as the image potential states is under progress.

Finally, we believe that present study will be useful for the interpretation of experiments on dynamics of electronic states in metal-overlayer/metal systems.

ACKNOWLEDGMENTS

We acknowledge fruitful discussions with E. Ogando. This work has been funded partially by the University of the Basque Country UPV/EHU (Grant No. GIC07IT36607), the Departamento de Educación del Gobierno Vasco, and the Spanish Ministerio de Ciencía y Technología (MCyT) (Grant No. FIS2007-66711-C02-01). The SGI/IZO-SGIker UPV/EHU (supported by the National Program for the Promotion of Human Resources within the National Plan of Scientific Research, Development and Innovation—Fondo Social Europeo, MCyT, and Basque Government) is gratefully acknowledged for generous allocation of computational resources.

[1] B. J. Hinch, C. Koziol, J. P. Toennies, and G. Zhang, Europhys. Lett. **10**, 341 (1989).
[2] J. Braun and J. P. Toennies, Surf. Sci. **384**, L858 (1997).
[3] R. Otero, A. L. Vázquez de Parga, and R. Miranda, Phys. Rev. B **66**, 115401 (2002).
[4] A. L. Vázquez de Parga, J. J. Hinarejos, F. Calleja, J. Camarero, R. Otero, and R. Miranda, Surf. Sci. **603**, 1389 (2009).
[5] P. Czoschke, H. Hong, L. Basile, and T.-C. Chiang, Phys. Rev. Lett. **93**, 036103 (2004).
[6] O. Pfennigstorf, A. Petkova, H. L. Guenter, and M. Henzler, Phys. Rev. B **65**, 045412 (2002).
[7] Y. Guo, Y.-F. Zhang, X.-Y. Bao, T.-Z. Han, Z. Tang, L.-X. Zhang, W.-G. Zhu, E. G. Wang, Q. Niu, Z. Q. Qiu, J.-F. Jia, Z.-X. Zhao, and Q.-K. Xue, Science **306**, 1915 (2004).
[8] M. M. Özer, J. R. Thompson, and H. H. Weitering, Nat. Phys. **2**, 173 (2006).
[9] D. Eom, S. Qin, M. Y. Chou, and C. K. Shih, Phys. Rev. Lett. **96**, 027005 (2006).
[10] C. Brun, I.-Po Hong, F. Patthey, I. Yu. Sklyadneva, R. Heid, P. M. Echenique, K. P. Bohnen, E. V. Chulkov, and W.-D. Schneider, Phys. Rev. Lett. **102**, 207002 (2009).
[11] C. M. Wei and M. Y. Chou, Phys. Rev. B **66**, 233408 (2002).
[12] F. K. Schulte, Surf. Sci. **55**, 427 (1976).
[13] E. Ogando, N. Zabala, E. V. Chulkov, and M. J. Puska, Phys. Rev. B **69**, 153410 (2004).
[14] E. Ogando, N. Zabala, E. V. Chulkov, and M. J. Puska, Phys. Rev. B **71**, 205401 (2005).
[15] J. H. Dil, J. W. Kim, S. Gokhale, M. Tallarida, and K. Horn, Phys. Rev. B **70**, 045405 (2004).
[16] J. H. Dil, J. W. Kim, Th. Kampen, K. Horn, and A. R. H. F. Ettema, Phys. Rev. B **73**, 161308(R) (2006).
[17] J. H. Dil, T. U. Kampen, B. Hülsen, T. Seyller, and K. Horn, Phys. Rev. B **75**, 161401(R) (2007).
[18] L. Aballe, C. Rogero, P. Kratzer, S. Gokhale, and K. Horn, Phys. Rev. Lett. **87**, 156801 (2001).
[19] P. S. Kirchmann, M. Wolf, J. H. Dil, K. Horn, and U. Bovensiepen, Phys. Rev. B **76**, 075406 (2007).
[20] S. R. Barman, P. Häberle, K. Horn, J. A. Maytorena, and A. Liebsch, Phys. Rev. Lett. **86**, 5108 (2001).
[21] G. Materzanini, P. Saalfrank, and P. J. D. Lindan, Phys. Rev. B **63**, 235405 (2001).
[22] Y. Jia, B. Wu, H. H. Weitering, and Z. Zhang, Phys. Rev. B **74**, 035433 (2006).
[23] P. M. Echenique, R. Berndt, E. V. Chulkov, Th. Fauster, A. Goldmann, and U. Höfer, Surf. Sci. Rep. **52**, 219 (2004).
[24] J. Kliewer, R. Berndt, E. V. Chulkov, V. M. Silkin, P. M. Echenique, and S. Crampin, Science **288**, 1399 (2000).
[25] L. Vitali, P. Wahl, M. A. Schneider, K. Kern, V. M. Silkin, E. V. Chulkov, and P. M. Echenique, Surf. Sci. **523**, L47 (2003).
[26] E. V. Chulkov, J. Kliewer, R. Berndt, V. M. Silkin, B. Hellsing, S. Crampin, and P. M. Echenique, Phys. Rev. B **68**, 195422 (2003).
[27] P. S. Kirchmann and U. Bovensiepen, Phys. Rev. B **78**, 035437 (2008).
[28] H. Petek and S. Ogawa, Prog. Surf. Sci. **56**, 239 (1997).
[29] M. Wolf, E. Knoesel, and T. Hertel, Phys. Rev. B **54**, R5295 (1996).
[30] L. Hedin and S. Lundqvist, Solid State Phys. **23**, 1 (1969).
[31] C. Corriol, V. M. Silkin, D. Sánchez-Portal, A. Arnau, E. V. Chulkov, P. M. Echenique, T. von Hofe, J. Kliewer, J. Kroger, and R. Berndt, Phys. Rev. Lett. **95**, 176802 (2005).
[32] R. O. Jones and O. Gunnarsson, Rev. Mod. Phys. **61**, 689 (1989).
[33] Y. Wang and J. P. Perdew, Phys. Rev. B **43**, 8911 (1991).
[34] D. M. Ceperley and B. J. Alder, Phys. Rev. Lett. **45**, 566 (1980).
[35] E. V. Chulkov, V. M. Silkin, and P. M. Echenique, Surf. Sci. **391**, L1217 (1997); **437**, 330 (1999).
[36] K. Würde, A. Mazur, and J. Pollmann, Phys. Rev. B **49**, 7679 (1994).
[37] J. P. Perdew, H. Q. Tran, and E. D. Smith, Phys. Rev. B **42**, 11627 (1990).
[38] H. B. Shore and J. H. Rose, Phys. Rev. Lett. **66**, 2519 (1991).
[39] E. V. Chulkov, Yu. M. Koroteev, and V. M. Silkin, Surf. Sci. **247**, 115 (1991).
[40] F. Baumberger, A. Tamai, M. Muntwiler, T. Greber, and J. Osterwalder, Surf. Sci. **532-535**, 82 (2003).
[41] Y.-F. Zhang, J.-F. Jia, T.-Z. Han, Z. Tang, Q.-T. Shen, Y. Guo, Z. Q. Qiu, and Q.-K. Xue, Phys. Rev. Lett. **95**, 096802 (2005).
[42] J. Mandel and S. F. McCormick, J. Comput. Phys. **80**, 442 (1989).
[43] M. Heiskanen, T. Torsti, M. J. Puska, and R. M. Nieminen, Int. J. Quantum Chem. **91**, 171 (2001).
[44] E. V. Chulkov, I. Sarría, V. M. Silkin, J. M. Pitarke, and P. M. Echenique, Phys. Rev. Lett. **80**, 4947 (1998).
[45] E. V. Chulkov, V. M. Silkin, and M. Machado, Surf. Sci. **482-485**, 693 (2001).
[46] A. G. Eguiluz, Phys. Rev. B **31**, 3303 (1985).
[47] V. M. Silkin, J. M. Pitarke, E. V. Chulkov, and P. M. Echenique, Phys. Rev. B **72**, 115435 (2005).
[48] A. G. Borisov, A. K. Kazansky, and J. P. Gauyacq, Phys. Rev. Lett. **80**, 1996 (1998).
[49] A. G. Borisov, A. K. Kazansky, and J. P. Gauyacq, Phys. Rev. B **59**, 10935 (1999).
[50] A. G. Borisov, A. K. Kazansky, and J. P. Gauyacq, Surf. Sci. **430**, 165 (1999).
[51] E. V. Chulkov, A. G. Borisov, J. P. Gauyacq, D. Sánchez-Portal, V. M. Silkin, V. P. Zhukov, and P. M. Echenique, Chem. Rev. (Washington, D.C.) **106**, 4160 (2006).
[52] R. Otero, A. L. Vázquez de Parga, and R. Miranda, Surf. Sci. **447**, 143 (2000).
[53] P. M. Echenique and J. B. Pendry, J. Phys. C **11**, 2065 (1978).
[54] P. M. Echenique and J. B. Pendry, Prog. Surf. Sci. **32**, 111 (1989).
[55] J. Osma, I. Sarría, E. V. Chulkov, J. M. Pitarke, and P. M. Echenique, Phys. Rev. B **59**, 10591 (1999).
[56] J. J. Quinn and R. A. Ferrell, Phys. Rev. **112**, 812 (1958).
[57] P. M. Echenique, J. M. Pitarke, E. V. Chulkov, and A. Rubio, Chem. Phys. **251**, 1 (2000).
[58] S. Crampin, S. De Rossi, and F. Ciccacci, Phys. Rev. B **53**, 13817 (1996).
[59] E. Ogando, N. Zabala, E. V. Chulkov, and M. Puska, J. Phys.: Condens. Matter **20**, 315002 (2008).
[60] A. G. Borisov, E. V. Chulkov, and P. M. Echenique, Phys. Rev. B **73**, 073402 (2006).